J Hum Genet (2005) 50:92–98
DOI 10.1007/s10038-004-0225-5

ORIGINAL ARTICLE

Naoko Iwasaki · Yukio Horikawa · Takafumi Tsuchiya
Yutaka Kitamura · Takahiro Nakamura
Yukio Tanizawa · Yoshitomo Oka · Kazuo Hara
Takashi Kadowaki · Takuya Awata · Masashi Honda
Katsuko Yamashita · Naohisa Oda · Li Yu
Norihiro Yamada · Makiko Ogata · Naoyuki Kamatani
Yasuhiko Iwamoto · Laura del Bosque-Plata
M. Geoffrey Hayes · Nancy J. Cox · Graeme I. Bell

Genetic variants in the calpain-10 gene and the development of type 2 diabetes in the Japanese population

Received: 14 September 2004 / Accepted: 10 December 2004 / Published online: 5 February 2005

Abstract Variation in the gene encoding the cysteine protease calpain-10 has been linked and associated with risk of type 2 diabetes. We have examined the effect of three polymorphisms in the calpain-10 gene (SNP-43, Indel-19, and SNP-63) on the development of type 2 diabetes in the Japanese population in a pooled analysis of 927 patients and 929 controls. We observed that SNP-43, Indel-19, and SNP-63 either individually or as a haplotype were not associated with altered risk of type 2 diabetes with the exception of the rare 111/221 haplogenotype (odds ratio (OR) = 3.53, $P = 0.02$). However, stratification based on the median age-at-diagnosis in the pooled study population (< 50 and ≥50 years) revealed that allele 2 of Indel-19 and the 121 haplotype were associated with reduced risk in patients with later age-at-diagnosis (age-at-diagnosis ≥50 years OR = 0.82 and 0.80, respectively; $P = 0.04$ and 0.02). Thus, variation in the calpain-10 gene may affect risk of type 2 diabetes in Japanese, especially in older individuals.

Keywords Association study · Age-at-diagnosis · Calpain-10 · Genetics · Polymorphism · Type 2 diabetes

Naoko Iwasaki, Yukio Horikawa and Takafumi Tsuchiya contributed equally to this work.

N. Iwasaki (✉) · M. Ogata · Y. Iwamoto
Diabetes Center, Tokyo Women's Medical University,
8-1 Kawada-cho, Shinjuku-ku,
Tokyo 162-8666, Japan
E-mail: niwasaki@dmc.twmu.ac.jp
Tel.: +81-3-33538111
Fax: +81-3-33581941

Y. Horikawa · L. Yu · N. Yamada
Laboratory of Molecular Genetics,
Department of Cell Biology,
Institute for Molecular and Cellular Regulation,
Gunma University, Maebashi, Japan

T. Tsuchiya · L. del Bosque-Plata · M. G. Hayes · N. J. Cox · G. I. Bell
Departments of Biochemistry and Molecular Biology,
Human Genetics and Medicine,
The University of Chicago,
Chicago, Illinois, USA

Y. Kitamura · T. Nakamura · N. Kamatani
Department of Statistical Genetics,
Institute of Rheumatology,
Tokyo Women's Medical University,
Tokyo, Japan

Y. Tanizawa
Division of Molecular Analysis of Human Disorders,
Department of Bio-Signal Analysis,
Yamaguchi University Graduate School of Medicine,
Ube, Japan

Y. Oka
Division of Molecular Metabolism and Diabetes,
Department of Internal Medicine,
Tohoku University, Sendai, Japan

K. Hara · T. Kadowaki
Department of Metabolic diseases,
Graduate School of Medicine and Faculty of Medicine,
University of Tokyo, Tokyo, Japan

T. Awata
Division of Endocrinology and Diabetes, Department of Medicine,
Saitama Medical School, Saitama, Japan

M. Honda
Shiseikai Daini Hospital, Tokyo, Japan

K. Yamashita
Seijin Igaku Medical Clinic, Tokyo, Japan

N. Oda
Department of Internal Medicine,
Fujita Health University School of Medicine,
Aichi, Japan

Introduction

The results of association and linkage studies indicate that multiple genes are involved in determining susceptibility to type 2 diabetes in Japanese with each gene making a modest contribution to overall risk (Seino et al. 2001; Mori et al. 2001, 2002; Iwasaki et al. 2003). The gene encoding the cysteine protease calpain-10 (CAPN10) was first found to be associated with risk of type 2 diabetes in studies carried out in Mexican Americans (Horikawa et al. 2000). Two recent meta-analyses and a large association study have confirmed that single nucleotide polymorphisms (SNP)-43 and SNP-44 are associated with a 1.19- and 1.17-fold increased risk, respectively, of type 2 diabetes (Weedon et al. 2003; Song et al. 2004). SNP-43 may be a functional polymorphism affecting transcriptional regulation of the calpain-10 gene (Horikawa et al. 2000; Baier et al. 2000). However, Indel-19 and SNP-63 are just tagging SNPs, and their effect on transcriptional regulation or other functions of calpain-10 are unknown. The effect of the core CAPN10 polymorphisms SNP-43, Indel-19, and SNP-63 on risk of type 2 diabetes in Japanese has been examined in three small studies (Daimon et al. 2002; Horikawa et al. 2003; Shima et al. 2003). The results suggest that variation in CAPN10 is not a major risk factor. However, these studies were not able to quantify the effect of CAPN10 on risk because of the small number of cases and controls in the individual studies. Here, we reexamine the role of the CAPN10 in the development of type 2 diabetes in the Japanese population.

Material and methods

Subjects

All subjects were Japanese. We studied three groups of cases and controls. The first group (study 1) included 205 unrelated subjects with type 2 diabetes recruited from the outpatient clinic in the Diabetes Center, Tokyo Women's Medical University and 208 unrelated normoglycemic subjects recruited from the Seijin Igaku Medical Clinic of Tokyo Women's Medical University using the following inclusion criteria: age >60 years, HbA1c $<5.6\%$, and no family history of diabetes. The second group (study 2) consisted of 281 unrelated normal glucose-tolerant (by oral glucose tolerance testing) subjects who were recruited at four outpatient clinics: Diabetes Center, Tokyo Women's Medical University ($n=50$); Third Department of Internal Medicine, Yamaguchi University ($n=121$); Department of Internal Medicine, University of Tokyo ($n=30$); and Shiseikai Daini Hospital, Tokyo ($n=80$). The third group of subjects (study 3) comprised 454 patients with type 2 diabetes and 192 nondiabetic controls who were recruited from Gunma University Hospital and affiliated hospitals and Fujita Health University School of Medicine. The genetic studies were approved by the institutional review board of each participating institution. Informed consent was obtained from all participants.

The pooled analyses included the datasets above as well as the data from three published studies: Daimon et al. 2002, SNP-43; Horikawa et al. 2003, SNP-43, Indel-19 and SNP-63; and Shima et al. 2003, SNP-43, Indel-19, and SNP-63.

Linkage disequilibrium (LD)

We examined the structure of the linkage disequilibrium (LD) in the CAPN10 region using the software package GOLD [graphical overview of linkage disequilibrium (Abecasis and Cookson 2000)] and a common set of 14 SNPs having a minor allele frequency ≥ 0.10 in diabetic ($n=30$) and nondiabetic subjects ($n=30$).

Genotyping

Genomic DNA was prepared from peripheral blood lymphocytes by standard procedures. We typed three polymorphisms in CAPN10: SNP-43, CAPN10-g.4852G>A (rs3792267); insertion/deletion (Indel)-19, CAPN10-g.7920 (32 bp-repeats) (rs3842570); and CAPN10-g.16378C>T (rs5030952) as described previously (Horikawa et al. 2003) or using TaqMan-based assays with custom probes/primers (Applied Biosystems, Foster City, CA, USA). Additional SNPs used for studies of LD in the CAPN10 region were genotyped using TaqMan technology. Previous studies have shown that the three core polymorphisms lead to four common haplotypes described as 111, 112, 121, and 221 (allele 1 or 2 at SNP-43, Indel-19, and SNP-63, respectively). The haplogenotypes were assigned by inspection of the genotypes at SNP-43, Indel-19, and SNP-63.

Statistical analyses

Polymorphisms were tested for deviation from Hardy-Weinberg equilibrium, heterogeneity in allele and genotype among studies and differences in allele, genotype, haplotype, and haplogenotype between groups using a chi-squared test. All P values are two sided.

Results

Haplotype structure across the CAPN10 region

The analysis of LD in the region of CAPN10 revealed a single region of strong LD (Fig. 1).

CAPN10 and SNP-43, and Indel-19 and SNP-63 are contained within this single LD block, which does not

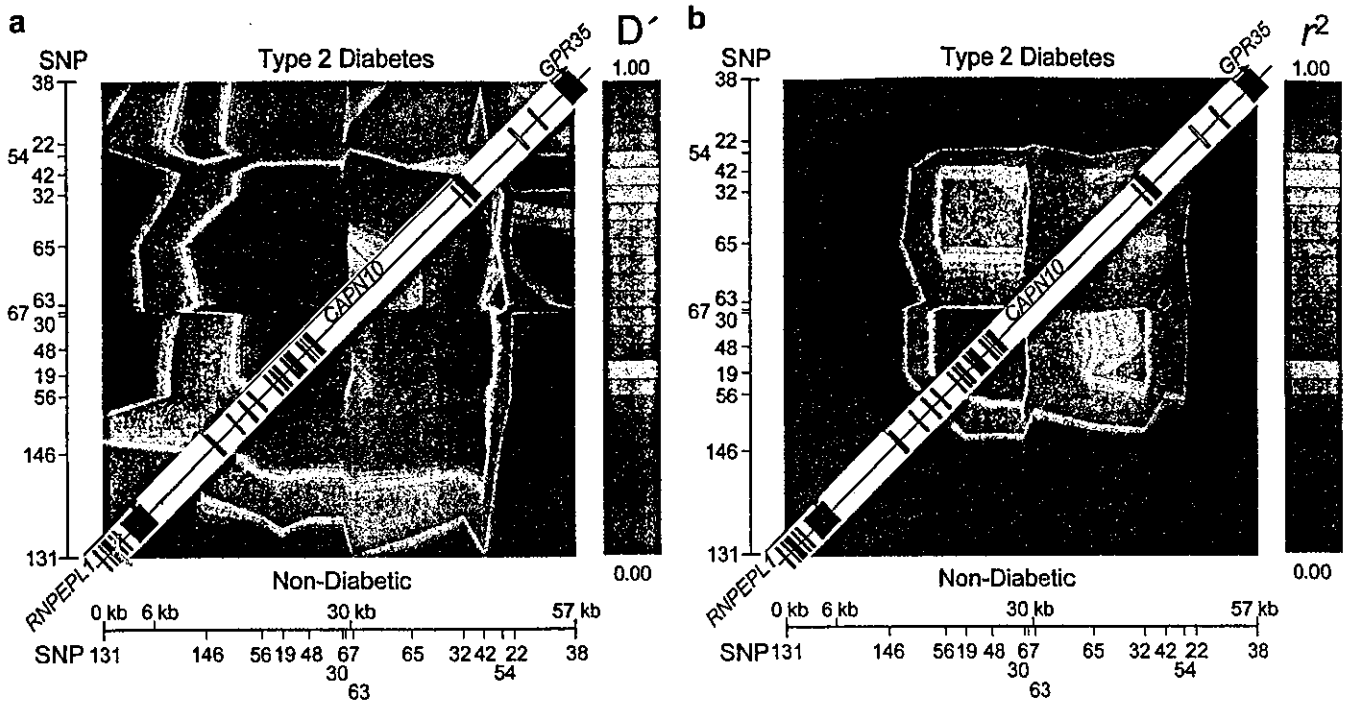

Fig. 1 Linkage disequilibrium (LD) in the CAPN10 region visualized using GOLD. The red and orange regions denote strong LD as defined using D' and r^2. The exons of CAPN10 and the adjacent genes RNPEPL1 and GPR35 are shown as *filled boxes* along the diagonal. The two variable number of tandem repeats (*VNTRs*) between CAPN10 and GPR35 are shown as *open boxes*. The SNPs used in this analysis are described in Horikawa et al. (2000). SNP-43 was not included in this analysis because the minor allele frequency was <0.10 in the Japanese population

include the flanking RNPEPL1 and GPR35 genes. Thus, association of polymorphisms in this block with type 2 diabetes or a type-2-diabetes-related trait in the Japanese population implies that it is a variation in CAPN10 itself and not an adjacent locus that is responsible for the effect. The associated variant may or may not be causal depending on the LD with other variants in the block.

Genetic variation in CAPN10 and type 2 diabetes

We typed SNP-43, Indel-19, and SNP-63 in the three study groups described above (Table 1). There was no significant difference in the frequency of SNP-43 or Indel-19 between cases and controls (Table 2), which is in agreement with previous studies in Japanese (Daimon et al. 2002; Horikawa et al. 2003). However, we observed a significant difference in SNP-63 allele frequency between cases and controls in the subjects from study 1 (0.66 and 0.73, respectively, $P=0.04$) but not in the subjects from study 3 (Table 2). In order to gain a better understanding of what role SNP-63 may play in the progression of type 2 diabetes, we examined the effect of SNP-63 genotype on various clinical and metabolic characteristics assessed by a standard 75-g oral glucose tolerance test in a group of 281 normal glucose-tolerant subjects from study 2 (Table 3). No significant effects of SNP-63 genotype on phenotype were observed except for area-under-the-curve plasma glucose level from 0 min to 120 min ($P=0.03$).

We then carried out a pooled analysis using data from all known studies carried out in the Japanese population (Daimon et al. 2002; Horikawa et al. 2003; Shima et al. 2003). The 281 nondiabetic subjects from study 2 were excluded from the primary analyses because their mean age-at-study in this group was significantly younger than other the control groups. The pooled study population included 927 patients and 929 controls although Indel-19 and SNP-63 were not typed in all subjects. There was no significant difference in SNP-43, Indel-19, or SNP-63 genotype or allele frequencies between the type 2 diabetic and control groups in the overall analysis (Table 4). There was also no significant difference in SNP-43/Indel-19/SNP-63 haplotype (Table 5) or haplogenotype frequency (Table 6) except for the rare 111/221 combination, which was associated with significantly increased risk of type 2 diabetes (OR = 3.53, $P=0.02$).

Genetic variation in CAPN10 may modify risk of type 2 diabetes in older patients

Since age is a risk factor for type 2 diabetes, we split the type 2 diabetic group based on median age-at-diagnosis, which was 50 years in the pooled sample, and repeated the comparisons but using only those cases for whom age-at-diagnosis was available: Patients with age-at-diagnosis <50 years included 118 patients from study 1, 103 from study 3, and 68 from Horikawa et al. (2003); and patients with age-at-diag-

Table 1 Clinical characteristics of study populations. Data are mean ± SD. *NA* data not available, *Ctrl* control, *T2D* type 2 diabetes

Trait	Study population											
	Study 1		Study 2		Study 3		Horikawa et al. (2003)		Shima et al. (2003)		Daimon et al. (2002)	
Subjects	Ctrl[a]	T2D	Ctrl	T2D	Ctrl[a]	T2D	Ctrl[a]	T2D	Ctrl	T2D	Ctrl	T2D
n	208	205	281	–	192	454	172	177	276	10	81	81
Gender (F/M)	68/140	84/121	135/146	–	70/122	206/248	90/82	63/114	NA	NA	46/35	45/36
Age-at-study (years)	67.9 ± 5.5	59.1 ± 13.0	44.4 ± 15.9	–	67.8 ± 5.6	59.9 ± 11.7	68.0 ± 5.7	62.0 ± 11.0	NA	NA	62.3 ± 8.2	65.1 ± 10.7
Age-at-diagnosis (years)	–	45.9 ± 12.7	–	–	–	51.0 ± 12.0[b]	–	49.8 ± 11.4	–	NA	–	NA
BMI	23.1 ± 2.4	23.5 ± 3.6	22.3 ± 3.0	–	23.1 ± 2.8	24.2 ± 4.2	22.8 ± 3.3	23.9 ± 3.3	NA	NA	23.8 ± 3.6	25.6 ± 3.9
HbA_{1c} (%)	5.0 ± 0.3	8.2 ± 2.0	4.9 ± 0.4	–	4.9 ± 0.3	7.9 ± 1.9	5.0 ± 0.4	6.7 ± 1.0	NA	NA	5.3 ± 0.3	6.7 ± 1.1
Fasting glucose (mg/dl)	95.0 ± 8.7	160.5 ± 48.5	92.8 ± 9.4	–	NA	NA	NA	NA	NA	NA	NA	NA
Treatment (diet/oral agents/insulin)	–	42/81/82	–	–	–	NA	–	46/70/61	–	NA	–	NA

[a] All subjects were > 60 years old
[b] Data are available for only 246 subjects

nosis ≥50 years included 87 patients from study 1, 143 from study 3, and 85 from Horikawa et al. (2003). There was no significant difference in SNP-43, Indel-19, and SNP-63 allele or genotype frequencies between the type 2 diabetic group with age-at-diagnosis < 50 years and the controls (Table 4). The SNP-43 and SNP-63 frequencies were also not different between the type 2 diabetic group with age-at-diagnosis ≥50 years and the controls. However, there was a small but significant difference in Indel-19 allele frequency (Table 4). The 3R allele at Indel-19 (allele 2 in the haplotype) was associated with lower risk of type 2 diabetes (OR = 0.82, $P = 0.04$).

The 121 haplotype was associated with significantly decreased risk (OR = 0.80, $P = 0.02$) of type 2 diabetes in the group of patients with age-at-diagnosis ≥50 years (Table 5). The 111 haplotype had the highest risk (OR = 1.33, $P = 0.046$) in the older group of patients. This effect of the 111 haplotype likely reflects the contribution of SNP-44 to type 2 diabetes risk (Weedon et al. 2003) since 88% of the 111 haplotypes in Japanese carry the at-risk C-allele at SNP-44. The rare 111/221 haplogenotype was associated with increased risk of type 2 diabetes irrespective of age-at-diagnosis (Table 6). The 121/121 haplogenotype had a protective effect against type 2 diabetes that approached significance in patients with age-at-diagnosis ≥50 years (OR = 0.76, $P = 0.06$). Individuals with haplotypes 111/111, 111/112, and 111/221 had the highest risk of type 2 diabetes (OR = 1.83, 1.25, and 4.12, respectively) although the increase in risk was not significant because of the small numbers of individuals studied. If the nondiabetic subjects in study 2 (Table 1) are included in the pooled control group, the results are similar, including the effects of the 121/121 haplogenotype on risk in patients with age-at-diagnosis ≥50 years (OR = 0.75, $P = 0.04$).

Discussion

The results suggest that genetic variation in CAPN10 may affect risk of type 2 diabetes in the Japanese population, especially in older individuals. Interestingly, the common 121 haplotype appears to be protective in Japanese, suggesting the overall effect of CAPN10 in this population is to reduce the risk of diabetes rather than increase it. It is important to note, though, that the statistical significance of the comparison is marginal ($P = 0.01$–0.04), and none of the comparisons would be significant if corrected for multiple testing. Thus, the results presented here need to be confirmed through studies of a much larger dataset. However, if our results are correct, they suggest an interaction between genetic (CAPN10) and nongenetic (age) factors to modify risk of type 2 diabetes. In this regard, recent studies have shown that calpain-10 is part of a novel apoptotic pathway in insulin-secreting pancreatic beta cells and thus may

Table 2 Genotype and allele frequencies of CAPN10 polymorphisms in Japanese. The number of subjects of each genotype are indicated. All genotypic distributions are in Hardy-Weinberg equilibrium. *NA* not available, *Ctrl* control, *T2D* type 2 diabetes

Marker	Subjects	Genotype	This study 1	This study 2	This study 3	Horikawa et al. (2003)	Shima et al. (2003)	Daimon et al. (2002)	*P* for heterogeneity
SNP-43	Ctrl	G/G	188	251	165	154	252	76	
		G/A	20	29	24	18	24	5	
		A/A	0	1	0	0	0	0	0.75
		Allele frequency	G: 0.95	G: 0.94	G: 0.94	G: 0.95	G: 0.96	G: 0.97	
			A: 0.05	A: 0.06	A: 0.06	A: 0.05	A: 0.04	A: 0.03	0.62
	T2D	G/G	184	NA	389	158	8	76	
		G/A	21	NA	57	19	2	5	
		A/A	0	NA	1	0	0	0	0.75
		Allele frequency	G: 0.95	NA	G: 0.93	G: 0.95	G: 0.90	G: 0.97	
			A: 0.05		A: 0.07	A: 0.05	A: 0.10	A: 0.03	0.37
Indel-19[a]	Ctrl	2R/2R	27	42	35	23	42	NA	
		2R/3R	99	126	78	78	126	NA	
		3R/3R	82	113	73	71	108	NA	0.90
		Allele frequency	2R: 0.37	2R: 0.37	2R: 0.40	2R: 0.36	2R: 0.38	NA	
			3R: 0.63	3R: 0.63	3R: 0.60	3R: 0.64	3R: 0.62		0.86
	T2D	2R/2R	32	NA	63	28	1	NA	
		2R/3R	104	NA	209	82	3	NA	
		3R/3R	69	NA	176	67	6	NA	0.62
		Allele frequency	2R: 0.41	NA	2R: 0.37	2R: 0.39	2R: 0.25	NA	
			3R: 0.59		3R: 0.63	3R: 0.61	3R: 0.75		0.34
SNP-63	Ctrl	C/C	111	151	99	90	151	NA	
		C/T	81	106	65	70	103	NA	
		T/T	16	24	18	12	22	NA	0.99
		Allele frequency	C: 0.73	C: 0.73	C: 0.72	C: 0.73	C: 0.73	NA	
			T: 0.27	T: 0.27	T: 0.28	T: 0.27	T: 0.27		0.99
	T2D	C/C	90	NA	255	93	6	NA	
		C/T	92	NA	165	74	3	NA	
		T/T	23	NA	30	10	1	NA	0.09
		Allele frequency	C: 0.66	NA	C: 0.75	C: 0.73	C: 0.75	NA	
			T: 0.34		T: 0.25	T: 0.27	T: 0.25		0.03

[a] Indel-19 is a diallelic insertion/deletion polymorphism with alleles of two repeats (2R) or three repeats (3R) of a 32-bp sequence

Table 3 Clinical and metabolic characteristics of normal glucose tolerant subjects (study 2) by SNP-63 genotype. Data are mean ± SD. Subjects underwent a standard 75-g oral glucose tolerance test with glucose and insulin determined at 0′, 30′, 60′, and 120′. The number of individuals in each group for determination of insulinogenic index and HOMA are noted in parentheses. *BMI* body mass index, *AUC* area under the curve

Trait	Genotype			P^a
	C/C	C/T	T/T	
n	150	105	25	
Gender (M/F)	72/78	59/46	14/11	0.40
Age (years)	45.0 ± 14.9	43.8 ± 16.7	44.4 ± 18.7	0.72
BMI (kg/m2)	22.3 ± 2.5	22.2 ± 3.6	22.6 ± 3.0	0.70
HbA1c (%)	4.9 ± 0.4	4.9 ± 0.4	5.0 ± 0.4	0.79
Plasma glucose (mg/dl)				
0 min	93.1 ± 9.6	92.2 ± 9.1	94.1 ± 8.8	0.51
120 min	104.1 ± 18.5	106.1 ± 18.8	108.2 ± 14.5	0.30
AUC 0-120′	14,510.6 ± 2706.2	15,233.4 ± 2937.1	15,043.2 ± 3056.1	0.03
Plasma insulin (μU/ml)				
0 min	6.4 ± 2.2	6.4 ± 2.6	6.5 ± 4.4	0.81
120 min	30.6 ± 16.9	32.0 ± 16.8	30.1 ± 20.2	0.74
AUC 0-120′	3,972.4 ± 2030.8	4,267.4 ± 1816.9	4,049.2 ± 1969.1	0.44
Insulinogenic index	0.89 ± 0.89 (147)	0.96 ± 3.62 (101)	1.14 ± 1.85 (24)	0.08
HOMA	1.43 ± 0.53 (146)	1.41 ± 0.54 (101)	1.30 ± 0.63 (23)	0.35

[a] *P* value by ANCOVA with institution, gender, and genotype as independent factors and age and BMI as covariates

affect the response of the beta cell to aging or its ability to compensate in response to an increasing demand for insulin (Johnson et al. 2004).

The observation that individuals homozygous for the 121 haplotype may be at increased risk of type 2 diabetes in some European populations (Orho-

Table 4 SNP-43, Indel-19, and SNP-63 and type 2 diabetes in Japanese—a pooled analysis. The number of subjects of each genotype are indicated. All genotypic distributions are in Hardy-Weinberg equilibrium. The cases were divided into two groups based on the median age-at-diagnosis in the pooled sample—50 years. Note that age-at-diagnosis was not available for all subjects

Marker	Genotype	Overall			Age-at-diagnosis < 50 years		Age-at-diagnosis ≥50 years	
		Ctrl	T2D	*P*	T2D	*P*	T2D	*P*
SNP-43	G/G	833	811		255		276	
	G/A	91	104		28	0.98	32	0.78
	A/A	0	1	0.35	0		0	
	Allele frequency	G: 0.95	G: 0.94		G: 0.95		G: 0.95	
		A: 0.05	A: 0.06	0.25	A: 0.05	0.98	A: 0.05	0.79
Indel-19[a]	2R/2R	127	124		36		58	
	2R/3R	381	396		143		151	0.11
	3R/3R	334	316	0.67	107	0.33	105	
	Allele frequency	2R: 0.38	2R: 0.39		2R: 0.38		2R: 0.43	
		3R: 0.62	3R: 0.61	0.69	3R: 0.62	0.91	3R: 0.57	0.04
SNP-63	C/C	451	443		149		151	
	C/T	319	333		125		129	
	T/T	68	62	0.72	14	0.09	28	0.35
	Allele frequency	C: 0.73	C: 0.73		C: 0.73		C: 0.71	
		T: 0.27	T: 0.27	0.94	T: 0.27	0.79	T: 0.29	0.17

[a] Indel-19: 2R, 2 repeats of 32-bp sequence; 3R, 3 repeats

Table 5 CAPN10 haplotype frequency and risk of type 2 diabetes in Japanese—a pooled analysis. The haplotypes are those defined by SNP-43, Indel-19, and SNP-63, and the specific alleles are: SNP-43, allele 1, G and allele 2, A; Indel-19, allele 1, 2 repeats of 32-bp sequence, and allele 2, 3 repeats; and SNP-63, allele 1, C, and allele 2, T. The cases were divided into two groups based on the median age-at-diagnosis in the pooled sample—50 years. Note that age-at-diagnosis was not available for all subjects. *Ctrl* control, *T2D* type 2 diabetes

Haplotype	Overall				Age-at-diagnosis < 50 years			Age-at-diagnosis ≥50 years		
	Ctrl ($n=825$)	T2D ($n=827$)	OR (95% CI)[a]	*P*	T2D ($n=277$)	OR (95% CI)[a]	*P*	T2D ($n=305$)	OR (95% CI)[a]	*P*
111	0.106	0.113	1.07 (0.86–1.34)	0.52	0.117	1.12 (0.83–1.52)	0.46	0.136	1.33 (1.00–1.75)	0.05
121	0.572	0.553	0.93 (0.81–1.07)	0.29	0.567	0.98 (0.81–1.19)	0.85	0.515	0.80 (0.66–0.96)	0.02
112	0.270	0.274	1.02 (0.88–1.19)	0.79	0.265	0.98 (0.78–1.21)	0.82	0.297	1.14 (0.93–1.40)	0.21
221	0.052	0.059	1.15 (0.85–1.54)	0.37	0.051	0.97 (0.62–1.50)	0.88	0.052	1.01 (0.66–1.53)	0.97

[a] The OR and 95% CI of each haplotype relative to other haplotypes as a group are shown

Table 6 CAPN10 haplogenotype and risk of type 2 diabetes in Japanese—a pooled analysis. The haplotypes are those defined by SNP-43, Indel-19, and SNP-63, and the specific alleles are indicated in the legend to Table 5. The number of individuals with each haplogenotype is indicated

Haplogenotype	Overall				Age-at-diagnosis < 50 years			Age-at-diagnosis ≥ 50 years		
	Ctrl	T2D	OR (95% CI)[a]	*P*	T2D	OR (95% CI)[a]	*P*	T2D	OR (95% CI)[a]	*P*
111/111	15	18	1.20 (0.60–2.40)	0.60	5	0.99 (0.36–2.76)	0.99	10	1.83 (0.82–4.07)	0.14
111/121	97	93	0.95 (0.70–1.29)	0.74	31	0.95 (0.62–1.45)	0.80	37	1.04 (0.69–1.55)	0.86
111/112	44	44	1.00 (0.65–1.53)	0.99	18	1.23 (0.70–2.17)	0.47	20	1.25 (0.72–2.15)	0.43
111/221	4	14	3.53 (1.24–10.1)	0.02	6	4.54 (1.42–14.5)	0.01	6	4.12 (1.27–13.3)	0.02
112/112	66	62	0.93 (0.65–1.34)	0.70	13	0.57 (0.31–1.04)	0.06	27	1.12 (0.70–1.78)	0.64
112/121	247	254	1.04 (0.84–1.28)	0.73	90	1.13 (0.84–1.51)	0.43	97	1.09 (0.82–1.45)	0.55
112/221	23	32	1.40 (0.82–2.41)	0.22	13	1.72 (0.86–3.41)	0.12	10	1.18 (0.56–2.51)	0.66
121/121	270	259	0.94 (0.76–1.15)	0.54	92	1.02 (0.77–1.37)	0.88	82	0.76 (0.56–1.01)	0.06
121/221	59	50	0.84 (0.57–1.23)	0.37	9	0.44 (0.22–0.87)	0.02	16	0.72 (0.41–1.27)	0.25
221/221	0	1	–	–	0			0		

[a] The OR and 95% CI of each haplogenotype relative to the other haplotype combinations as a group are shown

Melander et al. 2002; Malecki et al. 2002) but at decreased risk in older Japanese raises the possibility that additional genetic variation may distinguish high- and low-risk subtypes of the 121 haplotype. Transpopulation mapping may be a useful strategy for identifying this variation.

Acknowledgements The authors thank Ms. A. Nogami, Ms. M. Y. Sagisaka, and Mr. M. Ikeda for their skillful technical assistance. This study was supported by Grants-in-Aid for Scientific Research C (10671084, 10470234) and for Scientific Research on Priority Areas Medical Genome Science from the Japan Ministry of Science, Education, Sports, Culture and Technology (12204102, 13204082, 14013059, 15012250), Novo Nordisk Foundation, the Naito Foundation (to N.I.) and Grants-in-Aid for Scientific Research B (13470223, 13557091) (to Y.H.), and U.S. Public Health Service (Grants DK-20595, −47486 and −55889). G.I.B. is an Investigator of the Howard Hughes Medical Institute.

References

Abecasis GR, Cookson WO (2000) GOLD–graphical overview of linkage disequilibrium. Bioinformatics 16:182–183

Baier LJ, Permana PA, Yang X, Pratley RE, Hanson RL, Shen GQ, Mott D, Knowler WC, Cox NJ, Horikawa Y, Oda N, Bell GI, Bogardus C (2000) A 1-10 gene polymorphism is associated with reduced muscle mRNA levels and insulin resistance. J Clin Invest 106:R69-R73

Daimon M, Oizumi T, Saitoh T, Kameda W, Yamaguchi H, Ohnuma H, Igarashi M, Manaka H, Kato T (2002) Calpain-10 gene polymorphisms are related, not to type 2 diabetes, but to increased serum cholesterol in Japanese. Diabetes Res Clin Pract 56:147–152

Horikawa Y, Oda N, Cox NJ, Li X, Orho-Melander M, Hara M, Hinokio Y, Lindner TH, Mashima H, Schwarz PE, del Bosque-Plata L, Oda Y, Yoshiuchi I, Colilla S, Polonsky KS, Wei S, Concannon P, Iwasaki N, Schulze J, Baier LJ, Bogardus C, Groop L, Boerwinkle E, Hanis CL, Bell GI (2000) Genetic variation in the gene encoding calpain-10 is associated with type 2 diabetes mellitus. Nat Genet 26:163–175

Horikawa Y, Oda N, Yu L, Imamura S, Fujiwara K, Makino M, Seino Y, Itoh M, Takeda J (2003) Genetic variations in calpain-10 gene are not a major factor in the occurrence of type 2 diabetes in Japanese. J Clin Endocrinol Metab 88:244–247

Iwasaki N, Cox NJ, Wang YQ, Schwarz PE, Bell GI, Honda M, Imura M, Ogata M, Saito M, Kamatani N, Iwamoto Y (2003) Mapping genes influencing type 2 diabetes risk and BMI in Japanese subjects. Diabetes 52:209–213

Johnson JD, Han Z, Otani K, Ye H, Zhang H, Wu H, Horikawa Y, Misler S, Bell GI, Polonsky KS (2004) RyR2 and calpain-10 delineate a novel apoptosis pathway in pancreatic islets. J Biol Chem 279:24794–24802

Malecki MT, Moczulski DK, Klupa T, Wanic K, Cyganek K, Frey J, Sieradzki J (2002) Homozygous combination of calpain 10 gene haplotypes is associated with type 2 diabetes mellitus in a Polish population. Eur J Endocrinol 146:695–699

Mori H, Ikegami H, Kawaguchi Y, Seino S, Yokoi N, Takeda J, Inoue I, Seino Y, Yasuda K, Hanafusa T, Yamagata K, Awata T, Kadowaki T, Hara K, Yamada N, Gotoda T, Iwasaki N, Iwamoto Y, Sanke T, Nanjo K, Oka Y, Matsutani A, Maeda E, Kasuga M (2001) The Pro12 → Ala substitution in PPAR-γ is associated with resistance to development of diabetes in the general population: possible involvement in impairment of insulin secretion in individuals with type 2 diabetes. Diabetes 50:891–894

Mori Y, Otabe S, Dina C, Yasuda K, Populaire C, Lecoeur C, Vatin V, Durand E, Hara K, Okada T, Tobe K, Boutin P, Kadowaki T, Froguel P (2002) Genome-wide search for type 2 diabetes in Japanese affected sib-pairs confirms susceptibility genes on 3q, 15q, and 20q and identifies two new candidate Loci on 7p and 11p. Diabetes 51:1247–1255

Orho-Melander M, Klannemark M, Svensson MK, Ridderstrale M, Lindgren CM, Groop L (2002) Variants in the calpain-10 gene predispose to insulin resistance and elevated free fatty acid levels. Diabetes 51:2658–2664

Seino S on behalf of the Study Group of Comprehensive Analysis of Genetic Factors in Diabetes Mellitus (2001) S20G mutation of the amylin gene is associated with Type II diabetes in Japanese. Diabetologia 44:906–909

Shima Y, Nakanishi K, Odawara M, Kobayashi T, Ohta H (2003) Association of the SNP-19 genotype 22 in the calpain-10 gene with elevated body mass index and hemoglobin A1c levels in Japanese. Clin Chim Acta 336:89–96

Song Y, Niu T, Manson JE, Kwiatkowski DJ, Liu S (2004) Are variants in the CAPN10 gene related to risk of type 2 diabetes? A quantitative assessment of population and family-based association studies. Am J Hum Genet 74:208–222

Weedon MN, Schwarz PE, Horikawa Y, Iwasaki N, Illig T, Holle R, Rathmann W, Selisko T, Schulze J, Owen KR, Evans J, Del Bosque-Plata L, Hitman G, Walker M, Levy JC, Sampson M, Bell GI, McCarthy MI, Hattersley AT, Frayling TM (2003) Meta-analysis and a large association study confirm a role for calpain-10 variation in type 2 diabetes susceptibility. Am J Hum Genet 73:1208–1212

Available online at www.sciencedirect.com
SCIENCE DIRECT®
Cancer Letters 208 (2004) 115–122
CANCER Letters
www.elsevier.com/locate/canlet

Integrin-linked kinase (ILK) regulation of the cell viability in PTEN mutant glioblastoma and in vitro inhibition by the specific COX-2 inhibitor NS-398

Soichi Obara[a,b,*], Masanori Nakata[c], Hideo Takeshima[a], Hideki Katagiri[d], Tomoichiro Asano[e], Yoshitomo Oka[d], Ikuro Maruyama[b], Jun-ichi Kuratsu[a]

[a]*Faculty of Medicine, Department of Neurosurgery, Kagoshima University, 8-35-1 Sakuragaoka, Kagoshima 890-8520, Japan*
[b]*Faculty of Medicine, Department of Laboratory and Molecular Medicine, Kagoshima University, 8-35-1 Sakuragaoka, Kagoshima 890-8520, Japan*
[c]*Department of Physiology, Jichi Medical School, Minamikawachi, Kawachi, Tochigi 329-0498, Japan*
[d]*Division of Molecular Metabolism and Diabetes, Department of Internal Medicine, Tohoku University Graduate School of Medicine Seiryo-machi, Sendai, 980-8574, Japan*
[e]*Faculty of Medicine, Department of Internal Medicine, University of Tokyo, 7-3-1, Hongo, Bunkyo-ku, Tokyo 113-8655, Japan*

Received 10 November 2003; received in revised form 12 November 2003; accepted 13 November 2003

Abstract

We report the increased activity and expression of the ILK protein in human glioblastomas and demonstrate that ILK activity is regulated by PTEN. The transfection of wild type-PTEN into the glioblastoma cell line U-251 MG altered the localization of ILK in the cell membrane; transfection with PTEN down-regulated PKB/Akt-Ser-473 phosphorylation via the inhibition of ILK-signaling. Our results suggest that ILK is critical for the PTEN-sensitive regulation of PKB/Akt-dependent cell survival. The selective COX-2 inhibitor NS-398 was found capable of down-regulating ILK and PKB/Akt phosphorylation. Our data indicate that inhibition of ILK signaling may be beneficial in the treatment of PTEN-deficient glioblastoma.

Keywords: Glioblastoma; ILK; PTEN; PKB/Akt-Serine 473; NS-398

1. Introduction

Glioblastoma is the most common and the most malignant tumor of the human central nervous system. Despite extensive clinical trials, a good clinical outcome has remained an elusive goal [1,2]. The success of treatment is hampered by factors such as the rapid growth, remarkable genetic and biological heterogeneity, and high degree of infiltration of these neoplasms [3,4]. The mechanisms by which tumor cells survive apoptosis induced by cytotoxic treatment modalities remain unclear. Growth or angiogenic factors, cytokines, and a diverse array of parallel and overlapping signaling pathways are involved in

* Corresponding author. Address: Faculty of Medicine, Department of Neurosurgery, Kagoshima University, 8-35-1 Sakuragaoka, Kagoshima 890-8520, Japan. Tel.: +81-99-275-5437; fax: +81-99-275-2629.
E-mail address: sochian@ta2.so-net.ne.jp (S. Obara).

0304-3835/$ - see front matter © 2003 Elsevier Ireland Ltd. All rights reserved.
doi:10.1016/j.canlet.2003.11.020

the regulation of DNA repair and apoptosis. Identifying and ultimately targeting the molecules by which gliomas resist cytotoxic agents will have a strong impact on future treatment strategies.

PTEN, the phosphatase and tensin homolog deleted from chromosome 10, (also known as the mutated gene in multiple advanced cancers, MMAC1, and as the TGF-regulated and epithelial cell-enriched phosphatase, TEP1) was identified as a tumor suppressor gene located on chromosome 10q23 [5,6,7]. Loss of heterozygosity (LOH) at this locus is observed at a high frequency in a wide variety of human cancers including glioblastomas, melanomas, and carcinomas of the prostate, breast, lung, and head and neck [8–13]. PTEN is a lipid phosphatase that dephosphorylates 3D of phosphatidyliositol 3.4.5 triphosphate (PI (3, 4, 5) P3), a product of PI3-kinase. The disruption of PTEN results in the serum- and anchorage-independent activation of PKB/Akt probably induced by increased levels of PI (3, 4, 5) P3 [14–16]. PKB/Akt suppresses apoptosis via several possible downstream effectors including phosphorylation and inactivation of BAD [17], or repression of the forkhead transcription factor [18]. The disruption of PTEN leads not only to the suppression of apoptosis, but also to cell-cycle acceleration via GSK-3 and CyclinD [15].

Integrin-linked kinase (ILK) was identified by the yeast two-hybrid system as a serine/threonine kinase that interacts with the β1 integrin subunit [19]. ILK possesses a number of oncogenic properties including the inhibition of apoptosis and the acceleration of tumor cell invasion [20,21]. It has also been shown to phosphorylate PKB/Akt on Ser-473 in vitro. Since this activity is sensitive to the level of PI (3, 4, 5) P3 [22], the disruption of PTEN would be expected to activate ILK, leading to PKB/Akt activation [23]. In fact, ILK and PKB/Akt are constitutively activated in PTEN-mutant prostate cancer cells. Furthermore, the expression of dominant-negative ILK dramatically inhibits serum- and anchorage-independent PKB/Akt phosphorylation as well as PKB/Akt kinase activity, and leads to G1 cell-cycle arrest and enhanced apoptosis [24].

In the present work, we demonstrate that ILK is activated in PTEN-deficient human glioblastoma cells. We also found that transfection of WT-PTEN into these cells inhibits ILK activity, changes the subcellular localization of ILK, and ultimately inhibits PKB/Akt kinase activity, enhanced cell-cycle arrest, and apoptosis. Our results demonstrate that ILK is critical for the PTEN-sensitive regulation of PKB/Akt-dependent cell-cycle progression and cell survival. ILK kinase activity is suppressed by non-steroidal anti-inflammatory drugs (NSAIDs) [25]. Therefore, we exposed U-251MG cells to the COX-2-specific inhibitor NS-398. Interestingly, PKB/Akt-Ser-473 phosphorylation and the ILK activity were significantly inhibited by the administration of NS-398. Our data suggest that the inhibition of ILK-signaling by NSAIDs may have therapeutic benefits in PTEN-deficient glioblastomas since the restoration of PTEN by a viral vector is clinically difficult. Targeting the downstream of signal transduction pathways involved in the biology of tumor cells may represent a novel therapeutic approach.

2. Materials and methods

Brain tumor specimens and tumor cell lines. Glioma tissue specimens, obtained from patients who underwent surgery at The Department of Neurosurgery, Kagoshima University, were immediately frozen in liquid nitrogen. Sections from all samples were histologically evaluated by board-certified neuropathologists and classified according to the WHO grading system.

The human glioblastoma cell line U-251 MG was obtained as previously described [26]. The cell was cultured in Dulbecco's modified Eagle's medium (DMEM)(Gibco BRL, Grand Island, NY) supplemented with 10% fetal bovine serum at 37 °C in the presence of 95% air and 5% CO_2.

Gene expression. Recombinant Ade-XCA-PTEN has been described [27]. After infecting the U251 cells with DMEM containing adenovirus (30 min, 37 °C), DMEM containing 10% FCS was added. The adenovirus was applied at a MOI of 5–20 pfu/cell, and incubated for 48 h. Ade-XCA-lacZ was used as a control since on the three post-infection days, >90% of U251 cells exposed to a MOI of 10–20 pfu/cells manifested Ade-XCA-lacZ gene expression.

Immunohistochemistry. Histological sections (5-μm in thickness) of formalin-fixed, paraffin-embedded surgical specimens were subjected to

immunohistochemical staining. After incubation with normal blocking serum, the sections were incubated overnight at 4 °C with primary anti-ILK polyclonal antibody (0.2 μg/ml; Upstate Biotechnology, Lake Placid, NY). For immunodetection we employed the Vectastatin ABC rabbit IgG kit (Vector Laboratories, Burlingame, CA) using diaminobenzidine as the chromogen. Negative control sections were stained first with nonspecific rabbit IgG at the same protein concentration as the primary anti-ILK antibody, followed by horseradish peroxidase-linked anti-rabbit secondary antibody. All sections were counterstained with hematoxylin.

Immunoblot analysis. The cultured cells were collected and briefly sonicated in a Modified Radioimmunoprecipitation (RIPA) buffer containing 50 mM Tris (pH 7.4), 1% NP-40, 1 mM EDTA, 0.25% Na-deoxycholate, 1 mM PMSF, 1 mM NaF, and 1 mM Na_2VO_3, and a protease inhibitor cocktail (BD Pharminogen, San Diego, CA). The cell membranes were collected by a Mem-PER Mammalian Membrane Protein Extraction Reagent Kit (PIERCE, Rockford, IL). Frozen tissue samples were homogenized in RIPA buffer.

Immunoblot analysis using the enhanced chemiluminescence (ECL) detection system (Amersham Pharmacia, Little Chalfont Buckinghamshire, England) were carried out as described [19,22]. The following antibodies were used: anti-PTEN (goat polyclonal; Santa Cruz Biotech, Santa Cruz, CA); anti-ILK (affinity-purified rabbit polyclonal and mouse monoclonal antibody; Upstate Biotechnology, Lake Placid, NY); anti-PKB/Akt-phospho-Ser-473 (rabbit polyclonal; Transduction Laboratories, Lexington, KY); anti-PKB/Akt (mouse monoclonal; Transduction Laboratories).

ILK kinase assays. The ILK kinase activity was determined in cell extracts by immunoprecipitation kinase assays [21,22]. Glutathione S-transferase (GST)-PKB/Akt-Ser-473 was used as a substrate for ILK in separate experiments, and the phosphorylated proteins were electrophoresed on 12% SDS/PAGE gels. GST-PKB/Akt was constructed with individual GST fusion proteins of the PKB/Akt c-terminal (aa 444–480) expressed in JM109, and purified on glutathione-sepharose beads. When GST-PKB/Akt-Ser-473 was the substrate, [^{32}P]ATP was used as the phosphate donor in the kinase assay; [^{32}P]PKB/Akt-Ser-473 was detected by autoradiography or phosphorimage analysis of the gels. Cold ATP was the phosphate donor in kinase assays; the proteins were electrotransferred from SDS/PAGE gels to immobilize poly-(vinylidene difluoride) membranes (Millipore, Bedford, MA). Phosphorylated GST-PKB/Akt-Ser-473 was then detected by Western blot using anti-PKB/Akt-phospho-Ser-473 antibody.

Immunofluoresence microscopic analysis. The cells were maintained for 24 h on fibronectin-coated four-well chamber slides (Asahi Techno Glass, Tokyo, Japan), transfected with the adenovirus vectors, and fixed with 4% paraformaldehyde (10 min) followed by 0.1% Triton × 100 in PBS (5 min). After washing with PBS, they were stained with anti-ILK rabbit polyclonal antibody (Upstate Biotechnology) and anti-paxillin mouse monoclonal antibody (Transduction Laboratories). After again washing with PBS, the cells were incubated with the second antibody (30 min) and examined using a confocal laser scanning microscope (Leica True Confocal Scanner 4D, Leica Lasertechnik GmbH, Heidelberg, Germany) as described previously [28].

Cell viability. To assay cell viability, a modified dimethyl-2-thiazolyl-2,5 -diphenyl-tetrazolium bromide (MTT) assay. Briefly, glioblastoma cells, seeded at a density of $1.0–2.0 \times 10^5$ cells per 60 mm-dish, were transfected with WT-PTEN or control vector, and treated for 48 h with or without NS-398 (CALBIOCEM, Darmstadt, Germany).

3. Results

Since the expression profile of ILK has not been documented in glioma cells to date, we first determined the constitutive expression of ILK in glioma tissues obtained at surgery. In human glioma tissues, the level of ILK protein was higher than in normal brain. Furthermore, ILK expression was correlated with the malignancy grade of the gliomas (Figs. 1 and 2A). The most malignant type, glioblastoma, manifested a higher level of ILK expression than did low-grade gliomas.

The up-regulation of ILK in glioma tissues was histologically verified by immunohistochemical analysis. Vascular endothelial cells, smooth muscle cells,

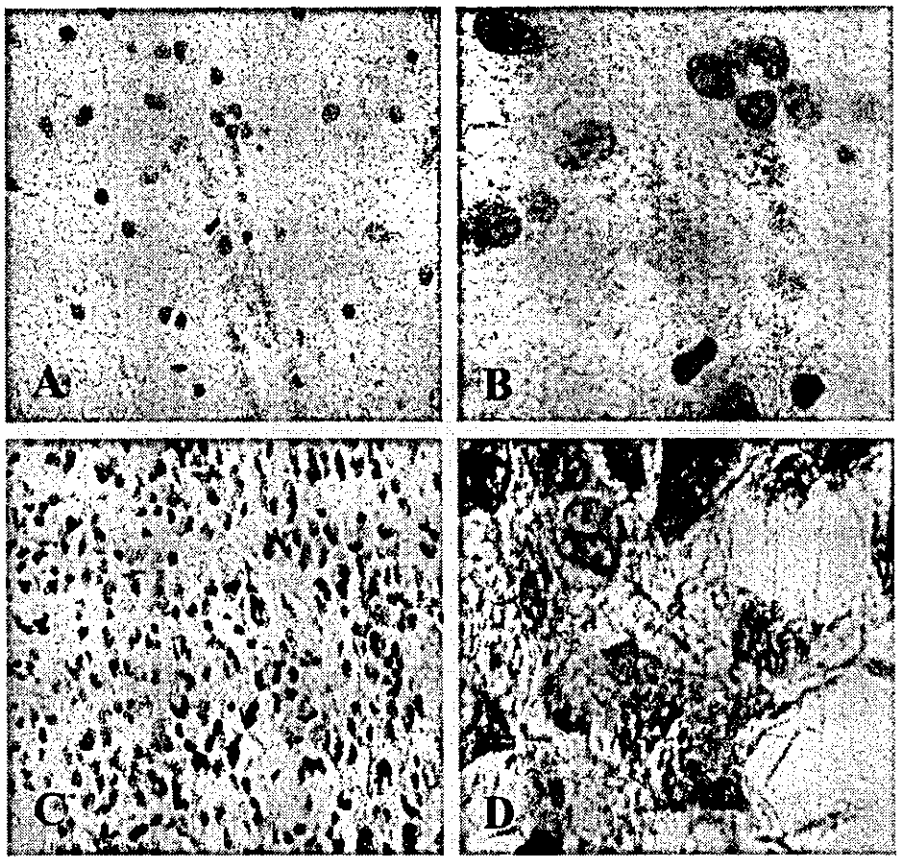

Fig. 1. Immunohistochemical detection of ILK in human glioma tissue. Low-grade astrocytoma and glioblastoma specimens were stained with primary anti-ILK polyclonal antibody followed by anti-rabbit secondary antibody. Vascular endothelial cells and pericytes were immunoreactive with anti-ILK antibody. Slight staining was detected in astrocytoma cells (A and B). Glioblastoma cells were stained strongly (C and D). Glioblastomas contained more ILK-positive cells than did low-grade astrocytomas. No staining was detected when control non-immune serum was used. Magnification: A and C × 200; B and D × 400.

and some tumor cells were immunoreactive with anti-ILK antibody in low-grade gliomas (Fig. 1A and B). On the other hand, the cytoplasm and cell surface were diffusely immunopositive for ILK in the majority of glioblastoma cells (Fig. 1C and D), suggesting that the increased level of ILK expression we observed was primarily attributable to the neoplastic glioma cells. In human glioma tissues, the level of ILK protein was higher than in normal brain. Furthermore, ILK expression was grossly correlated with the malignancy grade of the gliomas. The most malignant type, glioblastoma, manifested a higher level of ILK expression than low-grade gliomas by immunoblot analtysis (Fig. 2A).

To examine the biological relevance of ILK, PKB/AKT, and tumor suppressor PTEN in malignant glioma cells, we focused on how the PTEN status influenced the phosphorylation of PKB/AKT on Ser-473, and the expression level of ILK protein and it kinase activity. We experimented immunoprecipitated whole cell lysates with anti-ILK after transiently transfecting WT-PTEN into U-251 MG cells. Kinase assays using GST-PKB/AKT-C-terminal fusion protein as a substrate showed that restoration of PTEN leads not only to decreased PKB/AKT-Ser-473 phosphorylation but also to decreased ILK level and its activity (30% of mock stimulation; Fig. 2B and C).

As there is a direct association between ILK and paxillin with an LD1 motif, and co-localization in focal adhesions [29], we next examined whether decreased ILK activity affects the subcellular

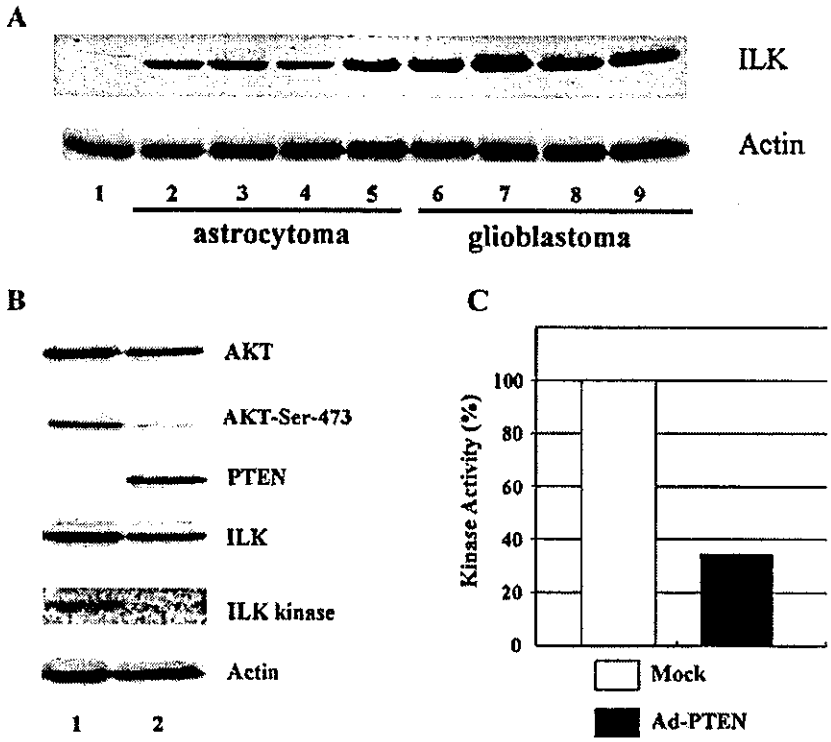

Fig. 2. Expression of ILK in glioma tissue specimens. Lane 1, normal human brain (CLONTECH). Lanes 2–5, human low-grade glioma tissues. Lanes 6–9, human glioblastoma tissues. The immunoblot with anti-actin (bottom) confirms equal loading of protein in each lane (A). Biological relevance of ILK, PKB/AKT, and tumor suppressor PTEN in malignant glioma cells. All cell lysates (500 mg protein) were immune-precipitated with anti-ILK antibody and kinase assays were performed using GST-PKB/AKT-C-terminal fusion protein as a substrate after transiently transfecting optimal MOI of PTEN adenovirus plasmid (20 MOI) into U-251 MG cells. Restoration of PTEN (lane 2) leads not only to decreased PKB/AKT-Ser-473 phosphorylation but also to decreased ILK level and its activity (30% of mock stimulation) (B). Densitometic analysis of ILK kinase. The intensity of immunoreactivity was measured by densitometry using the NIH-IMAGE image analysis software package (open bar, control adenovirus plasmid; solid bar, PTEN adenovirus plasmid) (C).

localization of ILK in glioblastoma cells. As expected, transfection with WT-PTEN not only inhibited ILK activity but also disrupted ILK localization on the cell membrane (Fig. 3A). To semi-quantitatively evaluate the shift of ILK from the cell membrane to the cytoplasm under different experimental conditions, we subjected equal amounts of membrane-bound and cytosolic proteins to immunoblot for ILK. As shown in Fig. 3B, a significant ILK shift from the membranous fraction to the cytoplasmic fraction was detected in PTEN-transfected U-251MG cells.

Restoration of PTEN produced cell-cycle arrest by inhibiting ILK activity in a variety of PTEN-deficient cell-lines such as prostate cancer lines [24]. Interestingly ILK activity has been shown to be inhibited by the administration of nonsteroidal anti-inflammatory drugs (NSAIDs) that can block both COX-1 and COX-2 [25]. Therefore, it is possible that the COX inhibitor suppresses the proliferation of glioma cells by inhibiting ILK activity regardless of the presence of wild-type PTEN.

We next compared the biological effect on cell proliferation of the specific COX-2 inhibitor NS-398 and of PTEN transfection. Interestingly, exposure to NS-398 (10 μM) resulted in a decrease in cell proliferation (Fig. 4A) that was comparable to that induced by PTEN-transfection. Immunoblot analysis demonstrated that phosphorylation of PKB/AKT-Ser-473 and ILK activities were significantly inhibited by cell exposure to NS-398 (Fig. 4B).

Our data demonstrate that in glioblastoma cells, like restoration of PTEN or exposure to NS-398, ILK induces decrease in cell proliferation. Therefore,

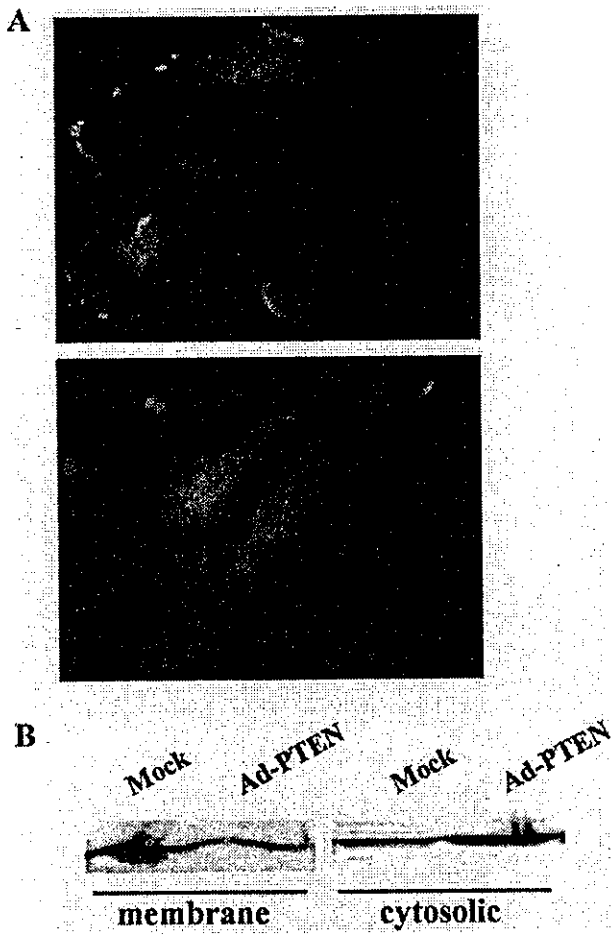

Fig. 3. Subcellular distribution of ILK. Immunofluorescence staining with ILK antibody of U-251 MG glioblastoma cells. After transfection with Mock Ad-LacZ, fluorescence-labeled ILK were identified in the cell membrane (upper panel). Transfection with Ad-PTEN resulted in disorganized ILK-staining in the cell membrane (lower panel) (A). Distribution of ILK in subcellular fractions of plasma membrane of U251 MG cells. Under different experimental conditions, equal amounts of membrane-bound and cytosolic proteins were Immunoblotted for ILK. Transfection with Ad-PTEN was associated with an attenuation of the presence of ILK in the membrane and its appearance in the cytoplasmic fraction (B).

the inhibition of ILK may represent a novel means of inhibiting the growth and progression of PTEN-mutant tumors.

4. Discussion

Increased ILK activity is correlated with the malignancy grade of several types of human tumors including breast, prostate, and colon carcinomas [30]. In the present work, we demonstrated the expression of ILK protein in human glioma cells. As shown by immunohistochemical and Immunoblot analysis, compared to low-grade gliomas, those of high grade expressed elevated levels of ILK protein. This is the first demonstration that in human glioblastoma cell line, ILK activity is constitutively activated. Furthermore, we found that the down-regulation of ILK activity by PTEN was related to changes in the localization of ILK from the cell membrane to the cytoplasm and ILK detached from focal adhesion plaques. ILK interacts with the cytoplasmic domains of β1 and β3 integrins via its C-terminal domain [31]. It was recruited to focal adhesions on extracellular matrix proteins and the kinase activity of ILK

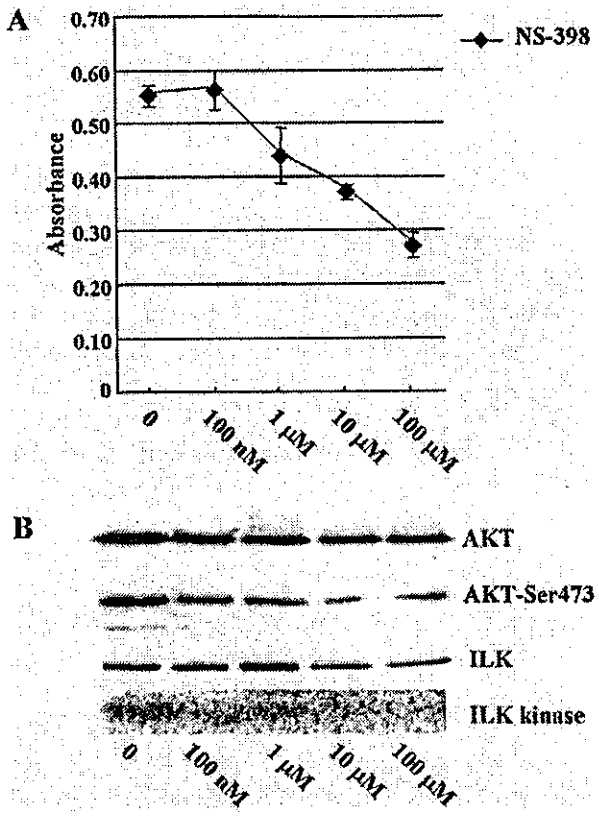

Fig. 4. Biological effect of the Cox2 inhibitor NS-398 in U-251 MG cells. To determine the MTT-induced reduction of cell viability, U-251 MG cells were incubated in 96-well microplates and exposed for 2 days to different concentrations of NS-398 (A). The results are given as the mean ± SD ($n = 3$). Immunoblot analysis of PKB/Akt-Ser-473 phosphorylation and in vitro kinase assay of ILK in NS-398-treated U-251 MG cells (B).

correlated with its anchoring on the cell membrane [29]. The activation of ILK in PTEN-null glioblastoma cells is presumably due to increased PI (3, 4, 5) P3 levels in these cells, although it is possible that ILK activation is due to dysregulation of other PTEN targets such as FAK [32]. Results from in vivo experiments suggested a role for PTEN in cell–cell and cell–matrix interactions and motility. Mouse embryos lacking PTEN exhibit severely disorganized blastocysts, suggesting that the expression of PTEN is required for proper cell–cell signaling. Furthermore, mutations in PTEN predominate in advanced invasive tumors and are present in about 72% of glioblastomas [33]. These findings suggest a role for PTEN in metastatic progression and are consistent with its putative role in adhesion and motility. As ILK overexpression resulted not only in cell transformation but also in increased metastasis in in vitro models [19,31,34,35], it is possible that ILK mediates many of the tumor suppressor functions of PTEN.

COX-2 is overexpressed in several tumor cells including glioma cells, and the COX-2 inhibitor suppressed the growth of these tumors [36,37]. Furthermore, ILK kinase activity was suppressed by NSAIDs such as ASA and Sulindac [25]. These lines of evidence suggest that the activation of ILK activity in cells containing COX-2 plays an important role in cell-cycle progression in these cells. Here we demonstrated that exposure of U-251MG cells to 20 μM NS-398 significantly inhibited ILK activity and PKB/AKT-Ser473 phosphorylation. Using the MTT cell proliferation assay, we also showed that tumor cell proliferation was inhibited.

Our findings indicate that the inactivation of a tumor suppressor results in the dysregulated activation of immediate downstream effectors. Their inhibition may represent selective and alternative means of treating tumors harboring mutations in the tumor suppressor genes. We demonstrated that the inhibition of ILK in glioblastoma cells induces decrease in cell proliferation. Our results suggest that the effects of ILK inhibition are specific for properties underlying malignant transformation. Therefore, targeting the ILK signal transduction pathways involved in the biology of glioblastoma cells may represent a therapeutic approach in the treatment of PTEN-deficient glioblastomas.

Acknowledgements

This research was supported in part by grants from the Ministry of Education, Science and Culture of Japan (to Masanori Nakata, Ikuro Maruyama, Jun-ichi Kuratsu, Yoshitomo Oka,) and a Jichi Medical School Young Investigator Award (to Masanori Nakata).

References

[1] F.W. Kreth, P.C. Warnke, R. Scheremet, C.B. Ostertag, Surgical resection and radiation therapy versus biopsy and radiation therapy in the treatment of glioblastoma multiforme, J. Neurosurg. 78 (1993) 762–766.

[2] F.W. Kreth, A. Berlis, V. Spiropoulou, M. Faist, R. Scheremet, R. Rossner, et al., The role of tumor resection in the treatment of glioblastoma multiforme in adults, Cancer 86 (1999) 2117–2123.

[3] D.C. Lyden, W.P. Mason, J.L. Finlay, The expanding role of chemotherapy for pediatric supratentorial malignant gliomas, J. Neurooncol. 28 (1996) 185–191.

[4] T.W. Trask, R.P. Trask, E. Aguilar-Cordova, H.D. Shine, P.R. Wyde, J.C. Goodman, et al., Phase I study of adenoviral delivery of the HSV-tk gene and ganciclovir administration in patients with current malignant brain tumors, Mol. Ther. 1 (2000) 195–203.

[5] D.M. Li, H. Sun, TEP1, encoded by a candidate tumor suppressor locus, is a novel protein tyrosine phosphatase regulated by transforming growth factor beta, Cancer Res. 57 (1997) 2124–2129.

[6] J. Li, C. Yen, D. Liaw, K. Podsypanina, S. Bose, S.I. Wang, et al., PTEN, a putative protein tyrosine phosphatase gene mutated in human brain, breast, and prostate cancer, Science 275 (1997) 1943–1947.

[7] P.A. Steck, M.A. Pershouse, S.A. Jasser, W.K. Yung, H. Lin, A.H. Ligon, et al., Identification of a candidate tumour suppressor gene, MMAC1, at chromosome 10q23.3 that is mutated in multiple advanced cancers, Nat. Genet. 15 (1997) 356–362.

[8] B.K. Rasheed, T.T. Stenzel, R.E. McLendon, R. Parsons, A.H. Friedman, H.S. Friedman, et al., PTEN gene mutations are seen in high-grade but not in low-grade gliomas, Cancer Res. 57 (1997) 4187–4190.

[9] W. Liu, C.D. James, L. Frederick, B.E. Alderete, R.B. Jenkins, PTEN/MMAC1 mutations and EGFR amplification in glioblastomas, Cancer Res. 57 (1997) 5254–5257.

[10] P. Guldberg, P. thor Straten, A. Birck, V. Ahrenkiel, A.F. Kirkin, J. Zeuthen, Disruption of the MMAC1/PTEN gene by deletion or mutation is a frequent event in malignant melanoma, Cancer Res. 57 (1997) 3660–3663.

[11] P. Cairns, K. Okami, S. Halachmi, N. Halachmi, M. Esteller, J.G. Herman, et al., Frequent inactivation of PTEN/MMAC1 in primary prostate cancer, Cancer Res. 57 (1997) 4997–5000.

[12] D.H. Teng, R. Hu, H. Lin, T. Davis, D. Iliev, C. Frye, et al., MMAC1/PTEN mutations in primary tumor specimens and tumor cell lines, Cancer Res. 57 (1997) 5221–5225.
[13] T. Kohno, M. Takahashi, R. Manda, J. Yokota, Inactivation of the PTEN/MMAC1/TEP1 gene in human lung cancers, Genes Chromosomes Cancer 22 (1998) 152–156.
[14] V. Stambolic, A. Suzuki, J.L. de la Pompa, G.M. Brothers, C. Mirtsos, T. Sasaki, et al., Negative regulation of PKB/Akt-dependent cell survival by the tumor suppressor PTEN, Cell 95 (1998) 29–39.
[15] H. Sun, R. Lesche, D.M. Li, J. Liliental, H. Zhang, J. Gao, et al., PTEN modulates cell cycle progression and cell survival by regulating phosphatidylinositol 3,4,5,-trisphosphate and Akt/protein kinase B signaling pathway, Proc. Natl Acad. Sci. USA 96 (1999) 6199–6204.
[16] S. Ramaswamy, N. Nakamura, F. Vazquez, D.B. Batt, S. Perera, T.M. Roberts, W.R. Sellers, Regulation of G1 progression by the PTEN tumor suppressor protein is linked to inhibition of the phosphatidylinositol 3-kinase/Akt pathway, Proc. Natl Acad. Sci. USA 96 (1999) 2110–2115.
[17] S.R. Datta, H. Dudek, X. Tao, S. Masters, H. Fu, Y. Gotoh, M.E. Greenberg, Akt phosphorylation of BAD couples survival signals to the cell-intrinsic death machinery, Cell 91 (1997) 231–241.
[18] A. Brunet, A. Bonni, M.J. Zigmond, M.Z. Lin, P. Juo, L.S. Hu, et al., Akt promotes cell survival by phosphorylating and inhibiting a Forkhead transcription factor, Cell 96 (1999) 857–868.
[19] G.E. Hannigan, C. Leung-Hagesteijn, L. Fitz-Gibbon, M.G. Coppolino, G. Radeva, J. Filmus, et al., Regulation of cell adhesion and anchorage-dependent growth by a new beta 1-integrin-linked protein kinase, Nature 379 (1996) 91–96.
[20] S. Attwell, C. Roskelley, S. Dedhar, The integrin-linked kinase (ILK) suppresses anoikis, Oncogene 19 (2000) 3811–3815.
[21] A.A. Troussard, P. Costello, T.N. Yoganathan, S. Kumagai, C.D. Roskelley, S. Dedhar, The integrin linked kinase (ILK) induces an invasive phenotype via AP-1 transcription factor-dependent upregulation of matrix metalloproteinase 9 (MMP-9), Oncogene 19 (2000) 5444–5452.
[22] M. Delcommenne, C. Tan, V. Gray, L. Rue, J. Woodgett, S. Dedhar, Phosphoinositide-3-OH kinase-dependent regulation of glycogen synthase kinase 3 and protein kinase B/AKT by the integrin-linked kinase, Proc. Natl Acad. Sci. USA 95 (1998) 11211–11216.
[23] S. Persad, S. Attwell, V. Gray, N. Mawji, J.T. Deng, D. Leung, et al., Regulation of protein kinase B/Akt-serine 473 phosphorylation by integrin-linked kinase: critical roles for kinase activity and amino acids arginine 211 and serine 343, J. Biol. Chem. 276 (2001) 27462–27469.
[24] S. Persad, S. Attwell, V. Gray, M. Delcommenne, A. Troussard, J. Sanghera, S. Dedhar, Inhibition of integrin-linked kinase (ILK) suppresses activation of protein kinase B/Akt and induces cell cycle arrest and apoptosis of PTEN-mutant prostate cancer cells, Proc. Natl. Acad. Sci. USA 97 (2000) 3207–3212.
[25] A. Marotta, C. Tan, V. Gray, S. Malik, S. Gallinger, J. Sanghera, et al., Dysregulation of integrin-linked kinase (ILK) signaling in colonic polyposis, Oncogene 20 (2001) 6250–6257.
[26] J. Kuratsu, K. Sato, Y. Saitoh, H. Takeshima, M. Morioka, Y. Ushio, The mechanism of growth-regulation of glioma cells by trapidil, J. Neurooncol. 23 (1995) 201–206.
[27] H. Ono, H. Katagiri, M. Funaki, M. Anai, K. Inukai, Y. Fukushima, et al., Regulation of phosphoinositide metabolism, Akt phosphorylation, and glucose transport by PTEN (phosphatase and tensin homolog deleted on chromosome 10) in 3T3-L1 adipocytes, Mol. Endocrinol. 15 (2001) 1411–1422.
[28] I. Kitajima, K. Kawahara, N. Hanyu, H. Shin, T. Tokioka, Y. Soejima, et al., Enhanced E-cadherin expression and increased calcium-dependent cell–cell adhesion in human T-cell leukemia virus type I Tax-expressing PC12 cells, J. Cell Sci. 109 (Pt3) (1996) 609–617.
[29] F. Li, Y. Zhang, C. Wu, Integrin-linked kinase is localized to cell-matrix focal adhesions but not cell-cell adhesion sites and the focal adhesion localization of integrin-linked kinase is regulated by the PINCH-binding ANK repeats, J. Cell Sci. 112 (Pt 24) (1999) 4589–4599.
[30] S.C. Wang, K. Makino, W. Xia, J.S. Kim, S.A. Im, H. Peng, et al., DOC-2/hDab-2 inhibits ILK activity and induces anoikis in breast cancer cells through an Akt-independent pathway, Oncogene 20 (2001) 6960–6964.
[31] G.E. Hannigan, J. Bayani, R. Weksberg, B. Beatty, A. Pandita, S. Dedhar, J. Squire, Mapping of the gene encoding the integrin-linked kinase, ILK, to human chromosome 11 p15.5–p15.4, Genomics 42 (1997) 177–179.
[32] M. Tamura, J. Gu, K. Matsumoto, S. Aota, R. Parsons, K.M. Yamada, Inhibition of cell migration, spreading, and focal adhesions by tumor suppressor PTEN, Science 280 (1998) 1614–1617.
[33] H. Lin, M.L. Bondy, L.A. Langford, K.R. Hess, G.L. Delclos, X. Wu, et al., Allelic deletion analyses of MMAC/PTEN and DMBT1 loci in gliomas: relationship to prognostic significance, Clin. Cancer Res. 4 (1998) 2447–2454.
[34] G. Radeva, T. Petrocelli, E. Behrend, C. Leung-Hagesteijn, J. Filmus, J. Slingerland, S. Dedhar, Overexpression of the integrin-linked kinase promotes anchorage-independent cell cycle progression, J. Biol. Chem. 272 (1997) 13937–13944.
[35] D.E. White, R.D. Cardiff, S. Dedhar, W.J. Muller, Mammary epithelial-specific expression of the integrin-linked kinase (ILK) results in the induction of mammary gland hyperplasias and tumors in transgenic mice, Oncogene 20 (2001) 7064–7072.
[36] T. Shono, P.J. Tofilon, J.M. Bruner, O. Owolabi, F.F. Lang, Cyclooxygenase-2 expression in human gliomas: prognostic significance and molecular correlations, Cancer Res. 61 (2001) 4375–4381.
[37] T. Joki, O. Heese, D.C. Nikas, L. Bello, J. Zhang, S.K. Kraeft, et al., Expression of cyclooxygenase 2 (COX-2) in human glioma and in vitro inhibition by a specific COX-2 inhibitor, NS-398, Cancer Res. 60 (2000) 4926–4931.

Available online at www.sciencedirect.com

SCIENCE DIRECT

European Journal of Pharmacology 502 (2004) 243–252

www.elsevier.com/locate/ejphar

Unique roles of G protein-coupled histamine H_2 and gastrin receptors in growth and differentiation of gastric mucosa

Yasushi Fukushima[a,*], Toshimitsu Matsui[b], Toshihito Saitoh[c], Masao Ichinose[d], Keisuke Tateishi[a], Takayuki Shindo[a], Midori Fujishiro[a], Hideyuki Sakoda[a], Nobuhiro Shojima[a], Akifumi Kushiyama[a], Satoru Fukuda[a], Motonobu Anai[a], Hiraku Ono[a], Masashi Oka[d], Yasuhito Shimizu[d], Hiroki Kurihara[a], Ryozo Nagai[a], Takashi Ishikawa[a], Tomoichiro Asano[a], Masao Omata[a]

[a]*Department of Internal Medicine, Graduate School of Medicine, University of Tokyo, 7-3-1 Hongo, Bunkyo-ku, Tokyo 113-8655, Japan*
[b]*Division of Hematology/Oncology, Department of Medicine, Kobe University School of Medicine, Kobe, Hyogo 650-0017, Japan*
[c]*Department of Internal Medicine, Tokyo Women's Medical University Daini Hospital, Arakawa-ku, Tokyo 116-8567, Japan*
[d]*Second Department of Internal Medicine, Wakayama Medical College, Kimiidera, Wakayama 640-0012, Japan*

Received 10 June 2004; received in revised form 20 August 2004; accepted 1 September 2004
Available online 1 October 2004

Abstract

Disruption of histamine H_2 receptor and gastrin receptor had different effects growth of gastric mucosa: hypertrophy and atrophy, respectively. To clarify the roles of gastrin and histamine H_2 receptors in gastric mucosa, mice deficient in both (double-null mice) were generated and analyzed. Double-null mice exhibited atrophy of gastric mucosae, marked hypergastrinemia and higher gastric pH than gastrin receptor-null mice, which were unresponsive even to carbachol. Comparison of gastric mucosae from 10-week-old wild-type, histamine H_2 receptor-null, gastrin receptor-null and double-null mice revealed unique roles of these receptors in gastric mucosal homeostasis. While small parietal cells and increases in the number and mucin contents of mucous neck cells were secondary to impaired acid production, the histamine H_2 receptor was responsible for chief cell maturation in terms of pepsinogen expression and type III mucin. In double-null and gastrin receptor-null mice, despite gastric mucosal atrophy, surface mucous cells were significantly increased, in contrast to gastrin-null mice. Thus, it is conceivable that gastrin-gene product(s) other than gastrin-17, in the stimulated state, may exert proliferative actions on surface mucous cells independently of the histamine H_2 receptor. These findings provide evidence that different G-protein coupled-receptors affect differentiation into different cell lineages derived from common stem cells in gastric mucosa.

Keywords: G protein; Histamine H_2; Double-null, mouse

1. Introduction

Recently, gene-targeting techniques have made it possible to generate mice deficient in a number of genes involved in gastric acid secretion (Friis-Hansen et al., 1998; Fukushima et al., 2003; Kobayashi et al., 2000; Koh et al., 1997; Langhans et al., 1997; Lloyd et al., 1997; Matsui et al., 2000; Nagata et al., 1996; Tanaka et al., 2002). Of these gene products, histamine H_2, gastrin, and muscarine M_3 receptors are direct targets of secretagogues and are involved in acid production in parietal cells. Targeted disruption of the histamine H_2 receptor caused hypertrophy of gastric mucosa due to marked hyperplasia of parietal, mucous neck and enterochromaffin-like (ECL) cells (Fukushima et al., 2003). Despite prominent hypergastrinemia, surface mucous cells were not as increased in number as downward migrating cells in histamine H_2 receptor-null mice (Fukushima et al., 2003). In contrast, gastrin receptor-null mice exhibited remarkable

* Corresponding author. Tel.: +81 3 3815 5411x33133; fax: +81 3 5803 1874.
E-mail address: fksm@mth.biglobe.ne.jp (Y. Fukushima).

0014-2999/$ - see front matter © 2004 Elsevier B.V. All rights reserved.
doi:10.1016/j.ejphar.2004.09.013

gastric mucosae atrophy accompanied by decreases in parietal and ECL cell numbers (Nagata et al., 1996). Although differences in pH values between wild-type mice and histamine H_2 receptor-null mice were minimal (Fukushima et al., 2003; Kobayashi et al., 2000), gastrin-dependent acid production was impaired in histamine H_2 receptor-null mice. In gastrin receptor-null mice, basal acid productions were lower than those in wild-type mice (Langhans et al., 1997; Nagata et al., 1996). In this study, to further clarify the distinct roles of histamine H_2 receptor and gastrin receptor in gastric mucosa, mice deficient in both the histamine H_2 and the gastrin receptors (double-null mice) were generated. We also analyzed gastric mucosa from aged histamine H_2 receptor-null mice and aged double-null mice. Herein, we present evidence that these different G-protein coupled-receptors mediate differentiation into different cell lineages derived from common stem cells in gastric mucosa.

2. Materials and methods

2.1. Mice

All animal experimental procedures were reviewed and approved by the Institutional Animal Care and Research Advisory Committee of the University of Tokyo. Mice deficient in histamine H_2 receptors were generated as described previously (Fukushima et al., 2003; Shindo et al., 2002).

2.2. Generation of mice deficient in both the histamine H_2 receptor and the gastrin receptor (double-null mice)

Histamine H_2 receptor-null mice and gastrin receptor-null mice with the genetic background of the 129/Sv×C57BL/6 hybrid were used (Fukushima et al., 2003; Nagata et al., 1996). Offspring obtained by crossing histamine H_2 receptor-null and gastrin receptor-null mice were confirmed to be heterozygous for both the histamine H_2 receptor and the gastrin receptor. These mice were then crossed and the offspring thus obtained were genotyped with PCR and/or Southern blot analysis using genomic DNA prepared from tail biopsies. Of these offspring, wild-type, histamine H_2 receptor-null, gastrin receptor-null and double-null mice were used for the following studies. Double-null mice appeared normal, were healthy into adulthood and both sexes were fertile.

2.3. Generation of polyclonal antibody against murine pepsinogen C

Polyclonal antibody against murine pepsinogen C was generated by a previously described method (Fukushima et al., 1993). The 100 carboxyl-terminal amino acids of murine pepsinogen C were fused to Glutathione *S*-transferase, which was used to immunize female New Zealand white rabbits. Serum collected from the immunized rabbits was passed through Affigel-10 beads, which had been cross-linked to Glutathione *S*-transferase. The flow-through was collected and passed through Afvfigel-10 beads, which had been cross-linked to the fusion protein. Antibody adsorbed to the beads was collected. This polyclonal antibody specifically recognizes chief cells in mouse oxyntic mucosa.

2.4. Histological analysis

Gastric specimens were fixed in 3% phosphate-buffered paraformaldehyde (pH 7.4), embedded in paraffin, and cut into 3 μm sections. The sections were stained with periodic acid-Schiff (PAS), hematoxylin and eosin, and examined under a light microscope. Paraffin-embedded gastric tissue sections were dewaxed and rehydrated with graded concentrations of ethanol. After treatment with 2% H_2O_2/phosphate buffered saline for 10 min, tissue sections were incubated with anti-pepsinogen C antibody, anti-histidine decarboxylase (HDC) polyclonal antibody, anti-$H^{(+)}/K^{(+)}$-ATPase monoclonal antibody (Fukushima et al., 1999), anti-type III mucin monoclonal antibody HIK1087 (Kanto-Kagaku, Japan) or normal rabbit or mouse immunoglobulin G (IgG) overnight at 4 °C. The sections were rinsed and then incubated for 30 min with biotinylated anti-rabbit or mouse IgG (1:400 dilution). The tissue sections were then rinsed and incubated for 30 min with peroxidase-labeled streptavidin (1:70 dilution). The slides were rinsed again in phosphate buffered saline and reacted with diaminobenzidine for 5 min at room temperature. Finally, the sections were rinsed and counterstained with hematoxylin.

2.5. Incorporation of the thymidine analog bromodeoxyuridine (BrdU)

BrdU (80 mg/kg BW(body weight)) was injected intraperitoneally into mice 2 h before sacrifice. Gastric tissues were removed and fixed in 3% phosphate-buffered paraformaldehyde. Immunohistochemistry with anti-BrdU monoclonal antibody was performed using paraffin-embedded sections from these samples.

2.6. Measurement of gastric pH

Wild-type and histamine H_2 receptor-null mice were fasted overnight with free access to water. At 1.5 h after subcutaneous injection of vehicle (0.5% methylcellulose), 10 mg/kg BW of famotidine, 10 mg/kg BW of pirenzepine dihydrochloride (a muscarine M_1 receptor antagonist) or 10 mg/kg BW of (*R*)-1-[2,3-dihydro-1-(2′ -methylphenacyl)-2-oxo-5-phenyl-1H-1,4-benzodiazepin-3-yl]-3-(3-methylphenyl)urea (YM022), a gastrin receptor antagonist, the mice were sacrificed and their stomachs were immediately excised. Gastric pH was measured using an ultra-thin pH monitor (Horiba, Japan).

2.7. Measurement of secretagogue induced acid secretion

Mice were maintained on anesthesia in chambers infused with oxygen gas saturated with diethylether. The stomach and duodenum were exposed via an epigastric midline incision. A tube inserted from the duodenum was placed in the gastric lumen. Stomachs were washed with 1 ml of prewarmed physiologic saline three times. After extraction of the tube and ligation of the pylorus, physiologic saline or secretagogue solution was administered peritoneally. A total of 10 mg/kg BW of histamine dihydrochloride, 0.05 mg/kg BW of carbachol or 0.1 mg/kg BW of gastrin-17 were administered, i.e. 2.5 ml/kg BW of physiologic saline as a control, histamine dihydrochloride solution (4 mg/ml), carbachol solution (0.02 mg/ml) or gastrin-17 solution (0.04 mg/ml). Thirty minutes after administration, the mice were sacrificed and their stomachs were excised. Gastric juice was collected with 1.5 ml of physiologic saline. Secreted gastric acid was measured by titrating the collected gastric juice to pH 7.0.

2.8. Statistical analysis

Quantitative values were expressed as means±S.E. Statistical significance was tested using the unpaired *t*-test (two tailed). A value of $P<0.05$ was considered significant.

3. Results

3.1. Comparison of gastric mucosae and serum gastrin levels of 10-week-old histamine H_2 receptor-null, gastrin receptor-null, double-null and wild-type mice

Stomachs from 10-week-old double-null mice weighed significantly less than those of 10-week-old wild-type mice (double-null 60.0±0.6 g/kg BW, wild-type 79.0±1.0 g/kg BW, $P<0.0001$). Macroscopically, oxyntic mucosae from double-null mice were more atrophic than those from wild-type mice (Fig. 1). Serum gastrin levels in double-null mice were significantly higher than those in wild-type mice, while being comparable to and lower than those in gastrin receptor-null mice and histamine H_2 receptor-null mice, respectively (Fig. 2). In addition, except in wild-type mice serum gastrin levels were not elevated by feeding (Fig. 2).

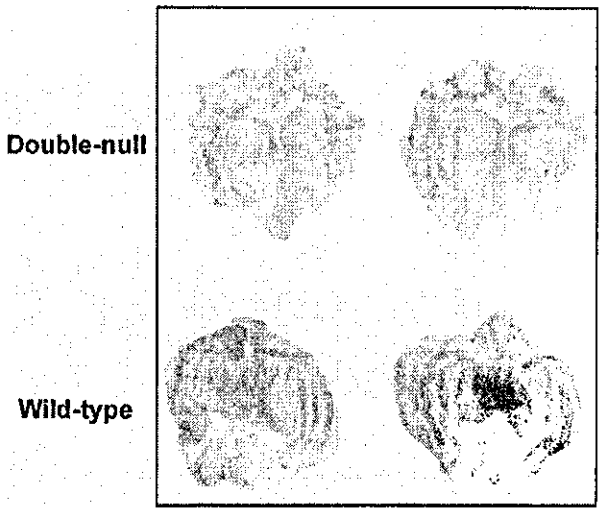

Fig. 1. Macroscopic views of stomachs from 10-week-old wild-type and double-null mice. The excised stomachs were opened along the greater curvature.

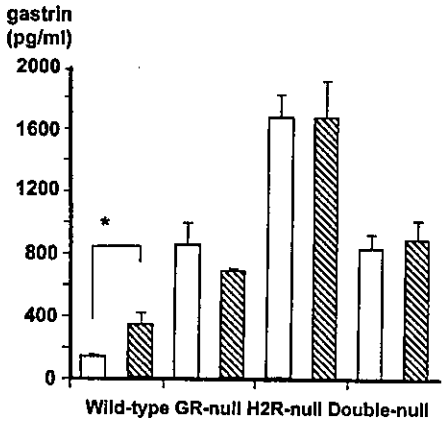

Fig. 2. Serum gastrin levels in wild-type, histamine H_2 receptor-null, gastrin receptor-null and double-null mice. Serum gastrin levels were measured in fasting (open bars) and fed states (hatched bars) in 10- to 12-week-old wild-type, histamine H_2 receptor-null (H2R-null), gastrin receptor-null (GR-null) and double-null mice. Data are presented as means±S.E. (n=15). *$P<0.0001$ between fasting and fed states.

To explore the effects of disrupting gastrin receptor and histamine H_2 receptor genes, we examined oxyntic mucosae from the four types of mice at 10 weeks of age, PAS staining of gastric mucosa from 10-week-old double-null mice showed no hypertrophy of oxyntic mucosae in double-null mice (Fig. 3D).

In histamine H_2 receptor-null mice, oxyntic mucosal hypertrophy was attributable to hyperplasia of ECL, parietal and mucous neck cells, and parietal cells were small (Table 1). In some portions of oxyntic mucosae from histamine H_2 receptor-null mice, peculiar mucous neck cells full of mucin protruded into the gastric gland lumen. Despite marked hypergastrinemia surface mucous cells were not as increased in number as the downward migrating cells, resulting in a decreased percentage of surface mucous cells per gland in histamine H_2 receptor-null mice. These findings confirm our previous report on histamine H_2 receptor-null mice (Table 1, Fig. 3B) (Fukushima et al., 2003). However, on closer examination, we found the number of surface mucous cells to be significantly increased as compared to wild-type mice (Table 1).

In gastrin receptor-null mice, numbers of downward migrating cells were decreased as previously reported ($P<0.001$, vs. wild-type mice) (Table 1) (Nagata et al., 1996). Interestingly, surface mucous cell cells were increased in number as compared with wild-type mice (26.7±1.6

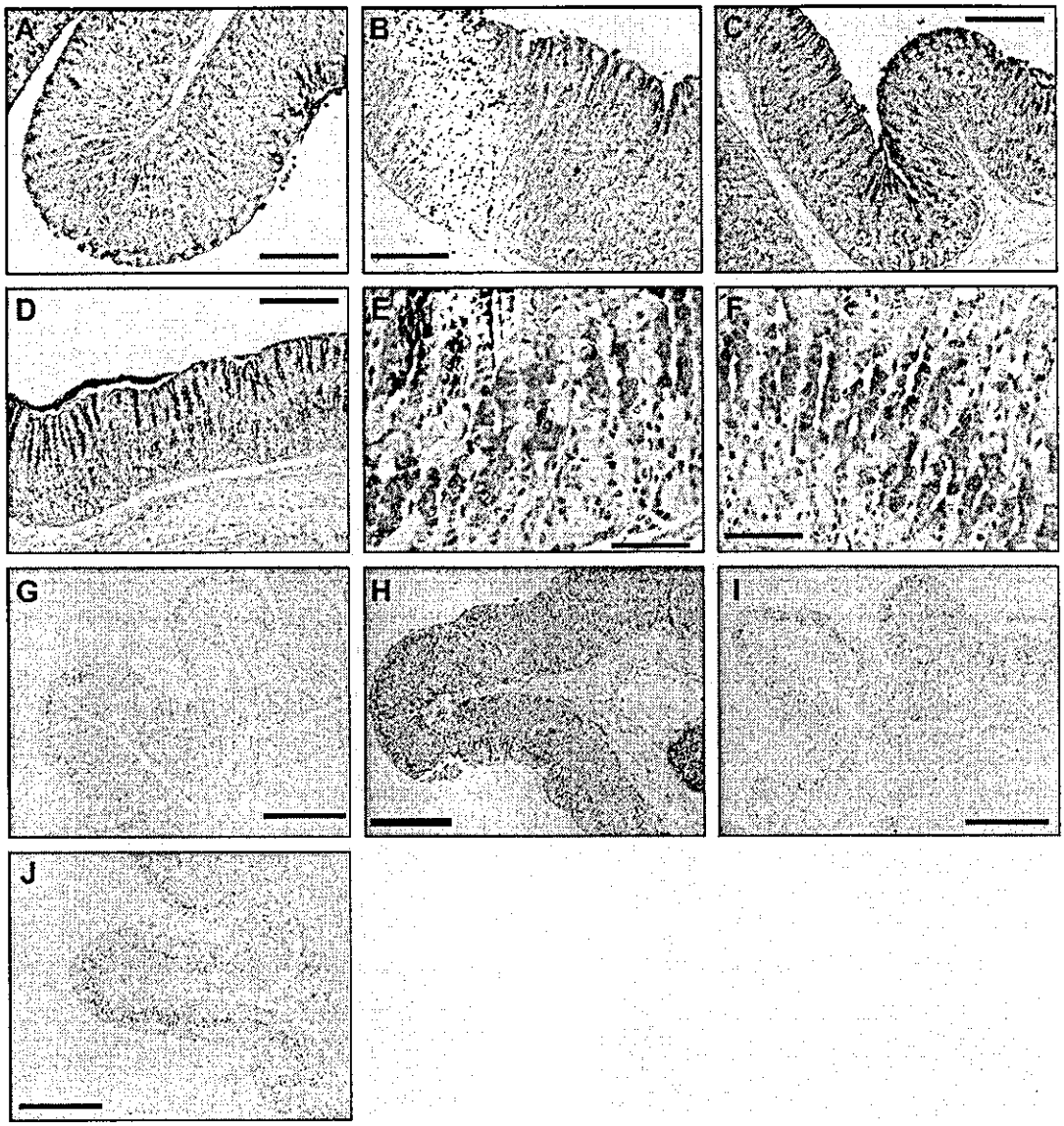

Fig. 3. Oxyntic mucosa from 10-week-old wild-type, histamine H_2 receptor-null, gastrin receptor-null and double-null mice. Sections of oxyntic mucosa from wild-type (A, G), histamine H_2 receptor-null (B, H), gastrin receptor-null (C, E, I) and double-null (D, F, J) mice were subjected to PAS staining (A, B, C, D, E, F) or BrdU labeling (G, H, I, J). Scale bars, 200 μm (A, B, C, D), 50 μm (E, F), 500 μm (G, H, I, J).

arbitrary units per gland vs. 20.3±0.5 arbitrary units per gland, $P<0.001$) (Table 1, Fig. 3C). Thus, although numbers of downward migrating cells were decreased, the total number of cells per gland did not differ significantly between gastrin receptor-null and wild-type mice (Table 1). In addition, an increase in the number of BrdU positive cells per gland was observed in gastrin receptor-null mice (gastrin receptor-null, 2.76±0.14 arbitrary units per gland, wild-type, 0.95±0.09 arbitrary units per gland, $P<0.001$) (Table 1, Fig. 3I). Just as in histamine H_2 receptor-null mice, some portions of the oxyntic mucosa, especially at the greater curvature and near the antrum, contained mucous neck cells full of mucins (Fig. 3E). Small parietal cells were observed in gastrin receptor-null mice as well (gastrin receptor-null mice, 5.37±0.10 arbitrary units per cell, wild-type mice, 8.86±0.17 arbitrary units per cell, $P<0.001$) (Table 1). In double-null mice, numbers of ECL cells, and parietal cells as well as the total number of downward migrating cells, were decreased (Table 1). As in gastrin receptor-null mice, the number of surface mucous cells was increased as compared with those from wild-type mice (25.3±0.8 arbitrary units per gland vs. 20.3±0.5 arbitrary units per gland, $P<0.001$) (Table 1, Fig. 3D). BrdU positive cells per gland were increased in number in double-null mice (double-null, 1.75±0.13 arbitrary units per gland, wild-type, 0.95±0.09 arbitrary units per gland, $P<0.001$) (Table 1, Fig. 3J). Total number of cells per gland did not differ significantly between wild-type and double-null mice (Table 1). Mucous neck cells with

Table 1
Quantitative analyses of gastric glands from 10-week-old wild-type, histamine H_2 receptor-null, gastrin receptor-null and double-null mice

	Total cell number	Surface mucous cell number	Gland cell number	Parietal cell		ECL cell number	BrdU positive cell number
				Number	Size		
Wild-type	63.7±0.7	20.3±0.5	43.4±0.7	20.3±0.4	8.86±0.17	1.44±0.13	0.95±0.09
Histamine H_2 receptor-null	114.2±3.6[a]	26.7±1.6[a]	87.5±2.9[a]	38.6±1.3[a]	4.79±0.11[a]	7.61±0.32[a]	2.01±0.11[a]
Gastrin receptor-null	61.5±1.2	26.7±0.7[a]	34.8±0.9[a]	13.8±0.2[a]	5.37±0.10[a]	0.53±0.08[a]	2.76±0.14[a]
Double-null	61.1±1.1	25.3±0.8[a]	35.8±0.8[a]	14.2±0.4[a]	5.01±0.09[a]	0.81± 0.07[a]	1.75±0.13[a]

Numbers of cells were counted in gastric glands sectioned centrally and in a manner parallel to their longitudinal axes, then expressed as arbitrary units per gland. Parietal cell size was determined by measuring the longitudinal cross sectional area of parietal cells from these gastric glands and expressed as arbitrary units per cell. One hundred glands from 10 mice (10 glands per mouse) were used for each type of mouse. Data are expressed as arbitrary units per gland or parietal cell since the data obtained are proportional but not equivalent to the actual cell numbers or parietal cell mass.

[a] $P<0.0001$ vs. wild-type mice.

characteristics similar to those in histamine H_2 receptor-null mice and gastrin receptor-null mice were seen in similar portions of the gastric mucosa (Fig. 3F). Small parietal cells were also observed in double-null mice (double-null mice, 5.01±0.09 arbitrary units per cell, wild-type mice, 8.86±0.17 arbitrary units per cell, $P<0.001$) (Table 1).

3.2. Comparison of chief cell lineage in gastric mucosae from 10-week-old wild-type, histamine H_2 receptor-null, gastrin receptor-null and double-null mice

Next, to explore the effects of histamine H_2 receptor and gastrin receptors on maturation of the chief cell lineage, expressions of pepsinogen and type III mucin were examined in gastric glands in each type of mouse. Fig. 4 is a schematic representation of a gastric gland. Fig. 5 shows that type III mucin positive cells were increased in number in histamine H_2 receptor-null, gastrin receptor-null and double-null mice as compared with wild-type mice. In addition, type III mucin positive cells, although present in the base regions of gastric glands from histamine H_2 receptor and double-null mice (Fig. 5J,L), were very scarce at the bases of gastric glands from wild-type and gastrin receptor-null mice (Fig. 5I,K). In wild-type mice, numbers of pepsinogen positive cells in gastric glands gradually increased from the isthmus to the base and pepsinogen expression per cell had already peaked in the neck region (Fig. 5A). In gastrin receptor-null mice, pepsinogen expression in gastric glands was maximal only at the base (Fig. 5C). It is noteworthy that mature chief cells, without type III mucin and with abundant pepsinogen, were present at the base region of gastric glands from gastrin receptor-null mice (Fig. 5C,G). In contrast, gland cells with abundant pepsinogen expression and without type III mucin were not present in histamine H_2 receptor-null mice and double-null mice (Fig. 5B,D,F,H). In addition to the low pepsinogen expression, pepsinogen levels per cell did not increase from the isthmus to the base in histamine H_2 receptor-null and double-null mice (Fig. 5B,D).

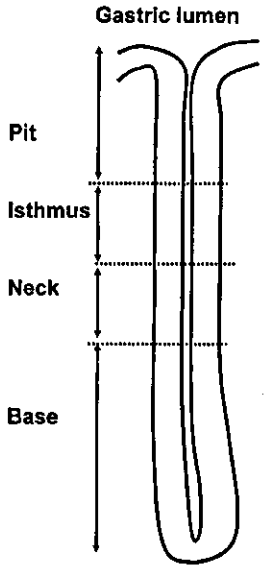

Fig. 4. Schematic drawing of a gastric gland.

3.3. Gastric pH and gastric acid productions in 10-week-old wild-type, histamine H_2 receptor-null, gastrin receptor-null and double-null mice

First, in vivo acid productions in response to secretagogues were measured. Histamine H_2 receptor-null mice were responsive to carbachol, but not to histamine or gastrin-17 (Fukushima et al., 2003). Secretagogue-induced acid secretion (10 mg/kg BW of histamine, 0.05 mg/kg BW of carbachol) was not observed in either gastrin receptor-null nor double-null mice (data not shown). Gastric pH values in double-null mice were the highest among the four types of mice (Fig. 6). Those in gastrin receptor-null mice were higher than those in wild-type or histamine H_2 receptor-null mice and lower than those in double-null mice. Treatment of gastrin receptor-null mice with famotidine (10 mg/kg BW) or pirenzepine (10 mg/kg BW) raised gastric pH values, indicating that histaminergic and muscarine pathways, although severely impaired, are functional in gastrin receptor-null mice. Because fasting gastric pH values in double-null mice were too high to assess the inhibitory effects of pirenzepine, the effect of